RAA 2015 Vol. **15** No. **1**, 28–36 doi: 10.1088/1674–4527/15/1/003
http://www.raa-journal.org *http://www.iop.org/journals/raa*

Research in Astronomy and Astrophysics

Variations of the harmonic components of the X-ray pulse profile of PSR B1509–58

Pragati Pradhan[1,2], Biswajit Paul[3], Harsha Raichur[3] and Bikash Chandra Paul[2]

[1] St Joseph's College, Singamari, Darjeeling 734104, West Bengal, India; *pragati2707@gmail.com*
[2] North Bengal University, Raja Rammohanpur, District Darjeeling 734013, West Bengal, India
[3] Raman Research Institute, Sadashivnagar, Bangalore 560080, India

Received 2013 November 27; accepted 2014 May 25

Abstract We used the Fourier decomposition technique to investigate the stability of the X-ray pulse profile of a young pulsar PSR B1509–58 by studying the relative amplitudes and phase differences of its harmonic components with respect to the fundamental using data from the Rossi X-Ray Timing Explorer. Like most young rotation powered pulsars, PSR B1509–58 has a high spin down rate. It also has less timing noise, allowing accurate measurement of higher order frequency derivatives which in turn helps in the study of the physics of pulsar spin down. Detailed investigation of pulse profiles over the years will help us establish any possible connection between the timing characteristics and the high energy emission characteristics for this pulsar. Furthermore, the study of pulse profiles of short period X-ray pulsars can also be useful when used as a means of interplanetary navigation. The X-ray pulse profile of this source has been analyzed for 15 yr (1996–2011). The long term average amplitudes of the first, second and third harmonics (and their standard deviation for individual measurements) compared to the fundamental are 36.9% (1.7%), 13.4% (1.9%) and 9.4% (1.8%) respectively. Similarly, the phases of the three harmonics (and standard deviations) with respect to the fundamental are 0.36 (0.06), 1.5 (0.2) and 2.5 (0.3) radian respectively. We do not find any significant variation of the harmonic components of the pulse profile in comparison to the fundamental.

Key words: pulsars: individual: (PSR B1509–58) — stars: neutron — X-rays

1 INTRODUCTION

With the launch of several sensitive space missions in the last two decades, the number of detected rotation-powered pulsars observable at X-ray energies has increased substantially. Pulsars with ages ranging from 10^3–7×10^9 yr, magnetic field strength ranging from 10^8–10^{13} G and spin periods ranging from 1.6–530 ms have been detected in X-rays (Becker & Truemper 1997). Rapid rotation coupled with strong magnetic fields of these pulsars results in a rotation-induced electric field which in turn accelerates the e^+–e^- pairs in the magnetosphere leading to high energy (γ-/X-ray) emission either by pair-photon cascades initiated by high energy photons above a polar cap (Ruderman & Sutherland 1975; Daugherty & Harding 1982, 1996) or in the outer gap (Cheng et al. 1986a,b; Hirotani 2008; Takata et al. 2010; Wang et al. 2010).

Owing to their fast rotation periods, magnetic fields of millisecond and young pulsars at their respective light cylinders are comparable even though the surface magnetic fields of the young pulsars are nearly five orders of magnitude larger than those of the former. This suggests to us that the magnetic field strength at the light cylinder may play a role in high energy emission in pulsars (Becker 2001).

Pulse profiles give us important information about the X-ray emission geometry of the pulsars. The average pulse profiles of pulsars, created by folding the light curve of the pulsars with their respective pulse period, exhibit predictable forms and are characteristic of every pulsar.

In young pulsars with ages less than 2000 yr such as the Crab pulsar, magnetospheric emission from charged particles accelerated in the neutron star magnetosphere along the curved magnetic field lines (Outer Gap model) dominate (Hirotani 2008). The magnetospheric component at X-ray energies is characterized by strong pulsations, sometimes with several peaked structures (Becker & Truemper 1997). Asymmetric pulse shapes indicate lack of axial symmetry in the emission zone. In millisecond pulsars like PSR 1821–24, 1937+21 and J0218+4232, the X-ray emission is dominated by non-thermal processes (Becker & Truemper 1997). Their pulse profiles have narrow peaks and a high pulsed fraction.

PSR B1509–58 was discovered in X-rays by the Einstein satellite (Seward & Harnden 1982), and later observations in radio (Manchester et al. 1982) confirmed its 150 ms period, giving it the highest spin-down rate, $\dot{P} \sim 1.5\times\ 10^{-12}$ s s^{-1}, of any known pulsar. It has a characteristic age nearly of 1700 yr, spin-down luminosity of $\dot{E}$ = 1.7 $\times\ 10^{37}$ erg s^{-1}, and dipole magnetic field of 1.5 $\times\ 10^{13}$ G. This magnetic field is larger than the magnetar SGR 0418+5729 which has the smallest magnetic field of less than 7.5 $\times\ 10^{12}$ G (Rea et al. 2010). Furthermore, its braking index, n, is less than 3, i.e, 2.839 $\pm$ 0.003 (Livingstone & Kaspi 2011). This could be due to the magnetic field being non-dipolar (Kaspi et al. 1994), or a result of pulsar wind that carries particles, taking angular momentum away from the pulsar causing resultant mass loss (Manchester et al. 1985). Some other reasons could be having a time variable effective magnetic moment (Blandford & Romani 1988) or a torque function, defined by $K = -\dot{\Omega}/\Omega^n$ where Ω is the spin rate of the pulsar, being time varying (Allen & Horvath 1997).

PSR B1509–58 was regularly observed between 1996 and 2011 with the Proportional Counter Array (PCA) (Jahoda et al. 1996, 2006) on board the Rossi X-ray Timing Explorer (RXTE). No glitches from this source have been observed so far, hence it gives us an opportunity to study the basic emission properties of this source over a long time without interruption. Also, no magnetar-like X-ray bursts were discovered in this pulsar.

Previous works on this pulsar showed that the X-ray component lags the radio component of the pulse by $\sim$ 0.27 period. The phase relation between the radio and the X-ray pulses, i.e. the difference in arrival time between the radio and the X-ray pulses, has been found to be quite stable (Livingstone et al. 2005). This lag is energy independent for the range 2–100 keV (Rots et al. 1998) suggesting that the radio and X-ray emission regions are different, favoring the Outer Gap model. This pulsar is known to emit radiations from radio to the soft-gamma region suggesting that there may be a new class of pulsars called soft-gamma ray pulsars (Pilia et al. 2010).

The timing studies of radio pulsars reveal that they are subjected to a systematic delay or spinning down. The measurements of the first and second time derivatives of pulsars' spin period can provide us with useful information about the dynamics of rotation for non-accreting neutron stars. The timing residuals for PSR B1509–58 from 1996–2010 show some significant structure. Also, while the braking index n is stable over long time scales, its variability is visible in short time scales (Livingstone & Kaspi 2011). This could well be due to changes in the magnetospheric activities of this pulsar, which may produce corresponding changes in the high energy X-ray emission. For PSR B1509–58, neither variability in X-ray flux nor any variability in pulse profile has been found when the pulse profiles were compared by using a χ^2 test, when upper limits for a change in flux of 28% were obtained (Livingstone & Kaspi 2011).

In this work we present our analysis of fifteen years of archival data of PSR B1509–58 observed using RXTE. The next section gives the details of the observations and the analysis techniques used; followed by Section 3 where we present the results. Then, in Section 4, we conclude with discussions on the obtained results.

2 OBSERVATION AND DATA ANALYSIS

The RXTE was launched on 1995 December 30. It was comprised of two instruments used for making pointed observations, the PCA in the energy range 2–60 keV and the High Energy X-ray Timing Experiment (HEXTE) covering the higher energy range 15–250 keV. In addition, RXTE carried an All-Sky Monitor (ASM) that scanned the sky. We used data obtained with the PCA (Jahoda et al. 1996). PCA is a collimated array of proportional counters, and is composed of five Proportional Counter Units (PCUs) with a total photon collection area of 6500 cm^2. Over the years, the average number of detectors available for observation decreased and the mission ended in early 2012.

For PSR B1509–58, archived RXTE-PCA data are available for 15 yr from 1996 to 2011 which enable us to study its timing characteristics in detail. We used data in Good Xenon mode that provides a full timing accuracy of about 1 μs. From the Science Event files recorded in Good Xenon mode, light curves were created using `seextrct` with a binning of 10 ms. The exposure times for the 262 observations used for this analysis were typically of the order of kiloseconds. Barycentric corrections were then made on the light curve that was created using `faxbary`. Using the ftools task `efsearch`, we find the best pulse period for each of the barycenter corrected light curves. One such period search is shown in Figure 1. Pulse profiles with 128 phase bins were created by folding the light curves with their respective best periods determined with a resolution of 10^{-7} s.

In order to choose the appropriate energy range, we first searched for the channel range with the maximum signal to noise ratio. The light curves were extracted for different energy intervals using an observation from 1996 and the respective pulse profiles were created. Each profile was fitted with a constant and the χ^2 value was noted. The greater the deviation was, the larger the value of χ^2 was, and hence the signal to noise ratio was greater. In this way, the channel and hence energy range was optimized for further analysis. The channel range optimization plot is given in Figure 2. The pulse

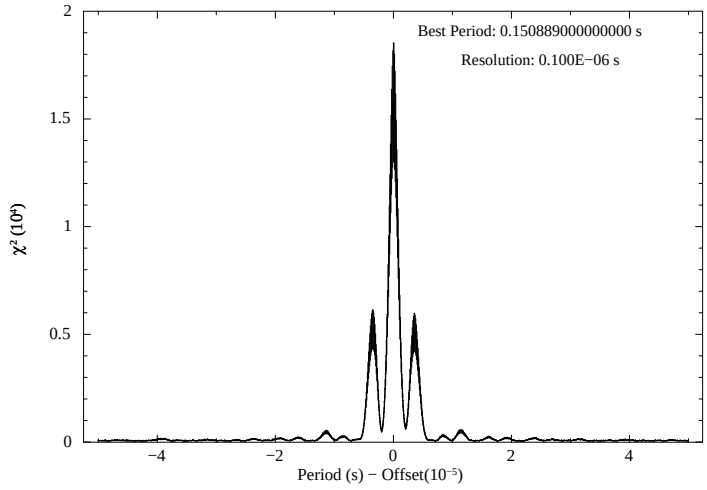

Fig. 1 The χ^2 in the pulse profile for different trial pulse periods is plotted here for a sample observation. The peak represents the true period.

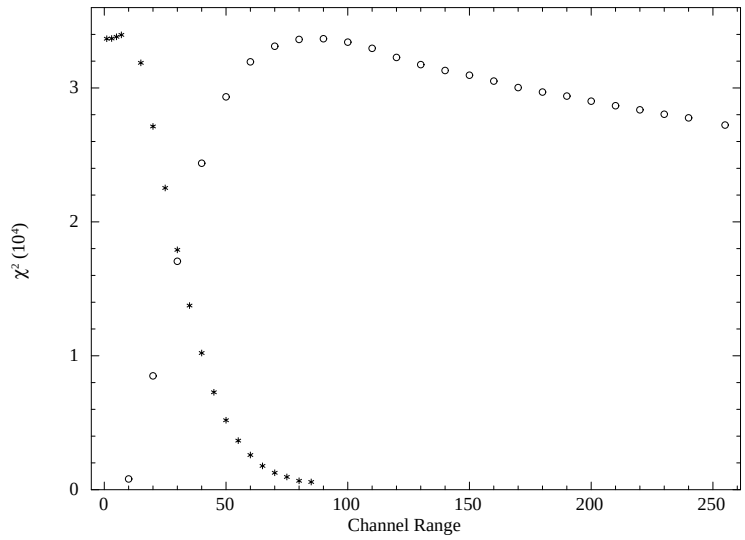

Fig. 2 Plot for optimization of Channel Range. The χ^2 of the folded light curve is plotted here for different channel ranges. For the circles, the X-axis represents the highest channel while the lowest channel is set to zero. This curve stops rising at about channel number 90. For the asterisks, the X-axis represents the lowest channel when the highest channel is fixed at 90. A channel range of 3–80 was selected for further analysis which will give the highest signal to noise ratio in the pulse profile.

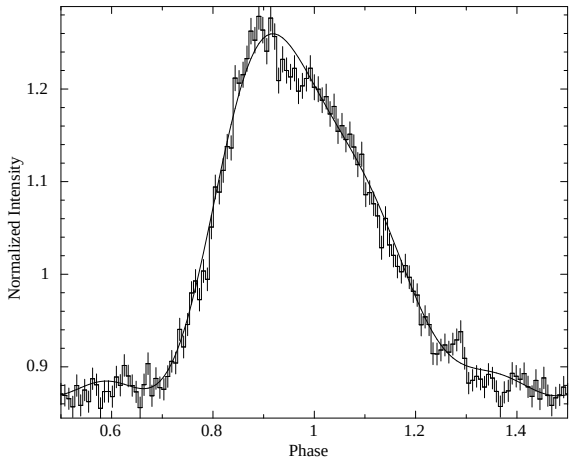

Fig. 3 A sample pulse profile in the energy range 2–24 keV. The pulse profile reconstructed by using the fundamental and the first three harmonics is overlayed.

profiles were created for all 262 observations taking the energy range to be $\sim$ 2 to 24 keV. A sample pulse profile is given in Figure 3.

Next, Fourier decomposition of the pulse profiles was carried out. The Fast Fourier Transform (FFT) method will decompose the signal from the pulsar into Fourier components and we get the amplitudes and phases of the frequency components, the sum of which make the individual pulse

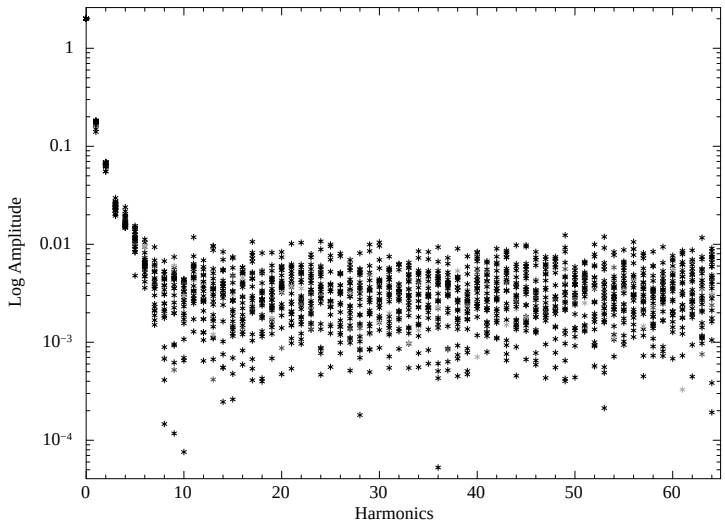

Fig. 4 Amplitudes of the harmonics are plotted here for 25 pulse profiles obtained from observations in 2004.

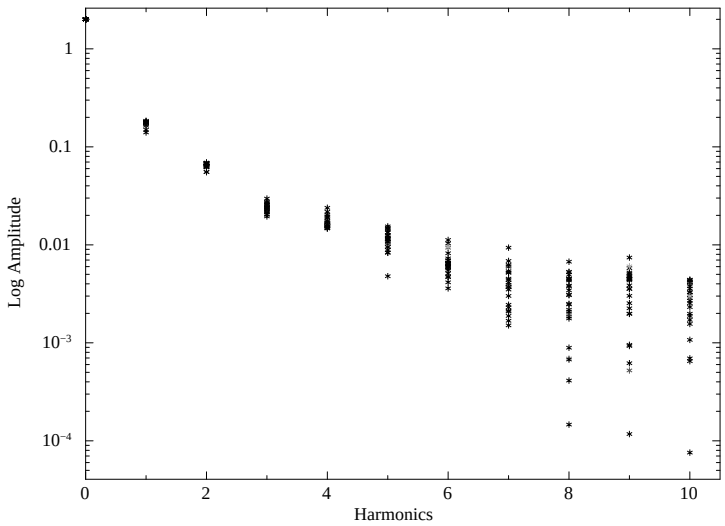

Fig. 5 Same as Fig. 4; only the first 10 harmonics are shown here.

profiles. It is then possible to calculate the relative amplitudes and the phase differences of the harmonics with respect to the fundamental for the pulse profile of all the years. Should the pulse profile remain unchanged, the relative amplitudes and phases of the harmonics with respect to the fundamental will be constant over time and will support the hypothesis that this pulsar has stable X-ray properties on long time scales.

Since the pulse profiles have limited statistics, there are definite uncertainties associated with measurement of the amplitudes and the phases. We have decomposed the individual pulse profiles into 128 Fourier components. In our analysis, we see that the first four Fourier components have the largest amplitudes and therefore have small relative errors, and are hence the most significant

components. We only compare these significant Fourier components. This is depicted in Figures 4 and 5.

Hence we make a comparison of the relative amplitudes and phase differences for the first three harmonics with respect to the fundamental. To make a comparison of phases, first the fundamental is shifted to zero, by subtracting it from itself. The first harmonic is shifted by twice the fundamental, second harmonic by thrice and the third harmonic by four times that. In this way the phase differences between the first, second and third harmonic and the fundamental are determined. We also calculate the ratio of the amplitudes of the first three harmonics with respect to the fundamental.

3 RESULTS

The relative amplitudes of the first, second and third harmonics and their fundamental for all the observations are shown in Figure 6 and the phase differences of the first three harmonics with respect to the fundamental in Figure 7. The long term average amplitudes of the first, second and third harmonics (and their standard deviation for individual measurements) compared to the fundamental are 36.9% (1.7%), 13.4% (1.9%) and 9.4% (1.8%) respectively. Similarly, the phases of the three harmonics (and standard deviations) with respect to the fundamental are 0.36 (0.06), 1.5 (0.2) and 2.5 (0.3) radian respectively.

To calculate the errors on the measured amplitudes and phases of the harmonics, we have carried out a Monte Carlo simulation. Pulse profiles were simulated with an intrinsic profile, the same as that shown with the solid line in Figure 3 but with a Gaussian deviation in each bin due to limited photon statistics. The same parameters were then measured from the simulated pulse profiles. The process was carried out 10 000 times and the standard deviation of each of the parameters obtained from the 10 000 simulations was taken to be the error on that parameter. The error obtained in a given pulse profile however depends on the total number of photons used to create the pulse profile. We have

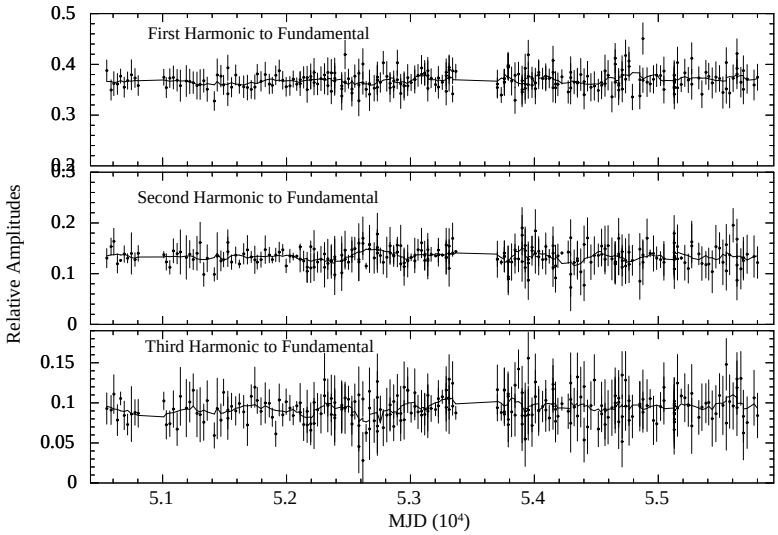

Fig. 6 The line represents the running mean over nine points of the relative amplitudes of the first three harmonics with respect to the fundamental while the points represent the actual values. The X-axis represents the MJD. The error bars were determined using the total number of photons in each pulse profile, results from a Monte Carlo simulation of the profiles and a scaling factor described in Section 3.

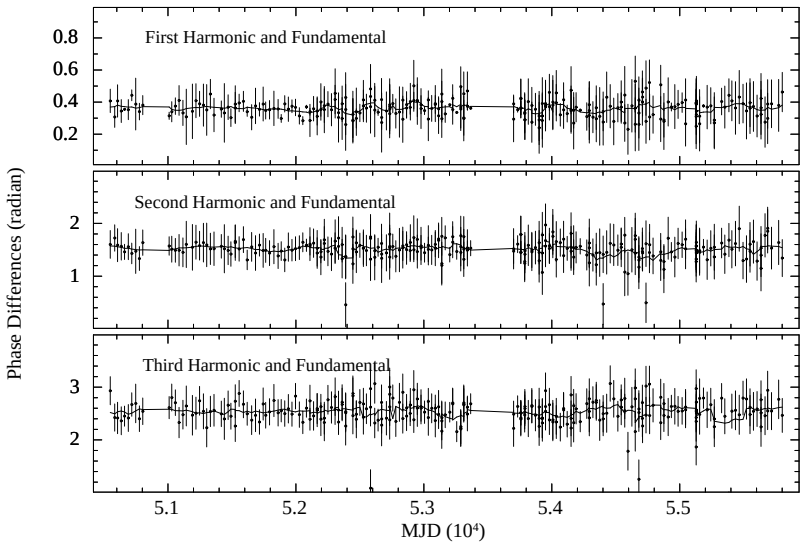

Fig. 7 The line represents the running mean over nine points of the phase difference of the first three harmonics and the fundamental while the points represent the actual values. The X-axis represents the MJD. The error bars are calculated in the same way as Fig. 6.

therefore estimated the dependence of the errors on the total number of photons used to create the pulse profiles by repeating the process for a different number of total photons. As expected, a power-law dependence with index –1/2 was found between the errors and the total number of photons. The total number of X-ray photons, which is known for each of the observations, was then used along with the above results to determine the error of the parameters for each of the observations. It was, however, found that there is a larger scatter in the measured parameters around the mean value compared to those obtained from the Monte Carlo simulation. We have measured the standard deviation of the parameters obtained from the 25 observations carried out in 2004 and obtained a scaling between the scatter and the errors estimated from the Monte Carlo simulation. All the error bars were multiplied by this scaling factor and are shown in Figures 6 and 7.

To investigate if there is an underlying trend, we have overplotted a nine point running average for each of the plots. The running mean indicates that on a longer timescale of about a year, there could be some systematic variation in the pulse profiles with an upper limit on percentage variation of the relative amplitudes of the first three harmonics to the fundamental being within 4%, 13% and 17% and phase differences of the first three harmonics from the fundamental being within 0.05, 0.15 and 0.14 radian of the respective long term averages. From Figures 6 and 7, it is also evident that there is a greater variation of phase difference and relative amplitudes from the mean for data taken with RXTE from the later years. This is probably due to the reduced sensitivity of the PCA resulting from loss of PCUs in the subsequent years of operation.

4 DISCUSSION

Pulsars show many types of flux variation on different time scales. Short term flux variations are generally bursts (Lewin et al. 1993) and glitches (Lyne et al. 1995).

No glitches have been observed for PSR B1509–58, but the younger Crab pulsar had 24 glitches in 42 yr (Espinoza et al. 2011) implying that the former has a higher internal temperature than the

latter (McKenna & Lyne 1990). Unlike the Crab and the Vela pulsar, PSR B1509–58 only exhibits an asymmetric, broad X-ray pulse suggesting that the X-ray pulse emission region is closer to a neutron star for PSR B1509–58 than for the other two (Kawai et al. 1991). The pulse profile analysis of PSR B1509–58 done here for the observations during the years 1996–2011 indicates some scatter in the amplitudes and phases. This is, however, not detectable by eye on pulse profiles.

It is worthwhile mentioning that the change in the radio pulse behavior of pulsars during time as short as their periods is solely considered to be a characteristic of radio emission. For the rotation powered pulsars, it is not possible to compare single X-ray pulses due to limited photon statistics. However, connection between the spin-down characteristics and the radio emission that is well known can also be probed for high energy emission. In this context, it is interesting to note the behavior of PSR B1931+24. This intermittent pulsar stopped emitting for days during during which time its rate of spin rapidly decreased by half (Young et al. 2013). For PSR J1841–0500 (Camilo et al. 2012) and PSR J1832+0029 (Lorimer 2007), changes in spin down rate are associated with variations in their average radio profiles. For PSR B1509–58, we are investigating if changes in the spin down characteristics are associated with any changes in the high energy emission properties.

We have made a quantitative estimate of any possible changes in the pulse profile by carrying out a Fourier decomposition and put upper limits of 36.9%, 13.4% and 9.4% on the amplitudes and 0.36, 1.5 and 2.5 radian on the phase of the first three harmonics with respect to the fundamental. A similar study of the pulse profile of the Crab pulsar, but using a different analytical expression for the profile, showed no pulse profile variation over a decade (Jain & Paul 2011).

The pulse profile stability of short period X-ray pulsars has an interesting application in interplanetary spacecraft navigation. By comparing the delay between the pulse arrival time measured onboard the spacecraft to the predicted arrival times in an inertial reference like the solar system barycenter, we can derive the relative position of the pulsar along the line of sight towards the pulsar. Three-dimensional information about the position of the spacecraft can be obtained likewise from the same information of at least three different pulsars (Bernhardt et al. 2010). This way, if we have a short period X-ray pulsar with a stable pulse profile, it can be used for navigation of spacecrafts. Also, decomposing the whole pulse profile into its Fourier components as discussed in this work has an advantage over only using the arrival time of the pulse peak (Sheikh et al. 2006).

Compared to millisecond pulsars, PSR B1509–58 is much slower and will not provide high position resolution needed for navigation. However, to be useful for the purpose of navigation, it is necessary for the X-ray pulse profile of rotation powered pulsars to be stable. After the Crab pulsar, PSR B1509–58 is the only bright source with many X-ray observations that can be used to investigate pulse profile stability. In the present work, we have given upper limits to its profile variation in terms of stability of the harmonic components with respect to the fundamental.

Acknowledgements The data for this work have been obtained through the High Energy Astrophysics Science Archive (HEASARC) Online Service provided by NASA/GSFC. Also, we thank the hospitality provided by the Raman Research Institute to PP and PP deeply thanks Chandreyee Maitra for her support in this analysis.

References

Allen, M. P., & Horvath, J. E. 1997, ApJ, 488, 409

Becker, W. 2001, X-ray Astronomy: Stellar Endpoints, AGN, and the Diffuse X-ray Background, 599, 13

Becker, W., & Truemper, J. 1997, A&A, 326, 682

Bernhardt, M. G., Prinz, T., Becker, W., & Walter, U. 2010, in Proceedings of High Time Resolution Astrophysics - The Era of Extremely Large Telescopes (HTRA-IV)

Blandford, R. D., & Romani, R. W. 1988, MNRAS, 234, 57P

Camilo, F., Ransom, S. M., Chatterjee, S., Johnston, S., & Demorest, P. 2012, ApJ, 746, 63

Cheng, K. S., Ho, C., & Ruderman, M. 1986a, ApJ, 300, 500
Cheng, K. S., Ho, C., & Ruderman, M. 1986b, ApJ, 300, 522
Daugherty, J. K., & Harding, A. K. 1982, ApJ, 252, 337
Daugherty, J. K., & Harding, A. K. 1996, ApJ, 458, 278
Espinoza, C. M., Lyne, A. G., Stappers, B. W., & Kramer, M. 2011, MNRAS, 414, 1679
Hirotani, K. 2008, ApJ, 688, L25
Jahoda, K., Markwardt, C. B., Radeva, Y., et al. 2006, ApJS, 163, 401
Jahoda, K., Swank, J. H., Giles, A. B., et al. 1996, in EUV, X-Ray, and Gamma-Ray Instrumentation for Astronomy VII, Society of Photo-Optical Instrumentation Engineers (SPIE) Conference Series, 2808, eds. O. H. Siegmund & M. A. Gummin, 59
Jain, C., & Paul, B. 2011, RAA (Research in Astronomy and Astrophysics), 11, 1134
Kaspi, V. M., Manchester, R. N., Siegman, B., Johnston, S., & Lyne, A. G. 1994, ApJ, 422, L83
Kawai, N., Okayasu, R., Brinkmann, W., et al. 1991, ApJ, 383, L65
Lewin, W. H. G., van Paradijs, J., & Taam, R. E. 1993, Space Sci. Rev., 62, 223
Livingstone, M. A., & Kaspi, V. M. 2011, ApJ, 742, 31
Livingstone, M. A., Kaspi, V. M., Gavriil, F. P., & Manchester, R. N. 2005, ApJ, 619, 1046
Lorimer, D. 2007, in Chandra Proposal, 2411
Lyne, A. G., Pritchard, R. S., & Shemar, S. L. 1995, Journal of Astrophysics and Astronomy, 16, 179
Manchester, R. N., Newton, L. M., & Durdin, J. M. 1985, Nature, 313, 374
Manchester, R. N., Tuohy, I. R., & Damico, N. 1982, ApJ, 262, L31
McKenna, J., & Lyne, A. G. 1990, Nature, 343, 349
Pilia, M., Pellizzoni, A., Trois, A., et al. 2010, ApJ, 723, 707
Rea, N., Esposito, P., Turolla, R., et al. 2010, Science, 330, 944
Rots, A. H., Jahoda, K., Macomb, D. J., et al. 1998, ApJ, 501, 749
Ruderman, M. A., & Sutherland, P. G. 1975, ApJ, 196, 51
Seward, F. D., & Harnden, F. R., Jr. 1982, ApJ, 256, L45
Sheikh, S. I., Pines, D. J., Ray, P. S., et al. 2006, Journal of Guidance Control Dynamics, 29, 49
Takata, J., Wang, Y., & Cheng, K. S. 2010, ApJ, 715, 1318
Wang, Y., Takata, J., & Cheng, K. S. 2010, ApJ, 720, 178
Young, N. J., Stappers, B. W., Lyne, A. G., et al. 2013, MNRAS, 429, 2569